



**HAL**  
open science

# Multilook phase difference distribution for slightly rough boundary layered ground

Saddek Afifi, Richard Dusséaux

## ► To cite this version:

Saddek Afifi, Richard Dusséaux. Multilook phase difference distribution for slightly rough boundary layered ground. *IET Microwaves Antennas and Propagation*, 2021, 15 (7), pp.718-727. 10.1049/mia2.12071 . insu-03205560v2

**HAL Id: insu-03205560**

**<https://insu.hal.science/insu-03205560v2>**

Submitted on 14 Jun 2021

**HAL** is a multi-disciplinary open access archive for the deposit and dissemination of scientific research documents, whether they are published or not. The documents may come from teaching and research institutions in France or abroad, or from public or private research centers.

L'archive ouverte pluridisciplinaire **HAL**, est destinée au dépôt et à la diffusion de documents scientifiques de niveau recherche, publiés ou non, émanant des établissements d'enseignement et de recherche français ou étrangers, des laboratoires publics ou privés.



Distributed under a Creative Commons Attribution - NonCommercial 4.0 International License

# Multilook phase difference distribution for slightly rough boundary layered ground

Saddek Affi<sup>1</sup> | Richard Dusséaux<sup>2</sup> 

<sup>1</sup>Electronics Department, Badji Mokhtar – Annaba University, Annaba, Algeria

<sup>2</sup>Laboratoire Atmosphères, Milieux, Observations Spatiales (LATMOS), Université de Versailles Saint-Quentin-en-Yvelines, Quartier des Garennes, Guyancourt, France

## Correspondence

Richard Dusséaux, Laboratoire Atmosphères, Milieux, Observations Spatiales (LATMOS), Université de Versailles Saint-Quentin-en-Yvelines, Quartier des Garennes, Guyancourt, France.  
Email: richard.dusseaux@latmos.ipsl.fr

## Funding information

National Key R&D Program of China, Grant/Award Number: 2016YFB0501503-3; National Natural Science Found, Grant/Award Number: 41730109

## Abstract

The authors derive the distribution of the phase difference between two multilook scattering signals for a multilayer stack with randomly rough surfaces under a plane wave excitation. First, for infinite slightly rough surfaces described by Gaussian centred stochastic processes, the authors show that the underlying complex scattering signals follow a Gaussian joint distribution. Also, it is demonstrated that this property is within the scope of the first-order perturbation theory. Secondly, the authors use this joint probability law to derive the closed-form expression for the probability density function of the phase difference. The theoretical formula is verified by comparison with Monte-Carlo simulations.

## 1 | INTRODUCTION

The phase difference between two complex scattering signals is an important parameter in the study of polarimetric data and it is related to the physical properties of the scattering medium under study [1–7]. To reduce statistical variations, it is often necessary to average data. The  $n$ -look phase difference is computed from a scattering matrix averaged over  $n$  single-look matrices. The probability laws for single-look and multilook phase differences have been found under the hypothesis of multivariate Gaussian scattering signals [8–15].

For a surface separating two homogenous media, the first-order small perturbation method (SPM) shows that the co-polarized and cross-polarized scattering signals are proportional to the Fourier transform of the surface height profile [16]. Therefore, the phase difference remains unchanged when the surface profile changes. But, for a stack of homogeneous dielectric layers with randomly rough surfaces under plane wave excitation, the ratios between the scattering signals depend on random surface profiles. For the two given incidence and observation directions, the co-polarized and cross-polarized phase differences are random variables. By using the

first-order SPM and by considering infinite slightly rough surfaces described by Gaussian centred stochastic processes, we showed in [16] that the probability density function (PDF) of the co-polarized phase difference for single-look configurations analysed in the incidence plane is a two-parameter distribution. This PDF only depends on the modulus  $r$  of the correlation coefficient between the two co-polarized complex signals with ( $0 \leq r \leq 1$ ) and on a reference angle  $\psi$ . When the two scattering signals are uncorrelated ( $r = 0$ ), the phase difference is uniformly distributed between  $0$  and  $2\pi$ . For fully correlated scattering signals ( $r = 1$ ), the phase difference is a deterministic quantity. Therefore, when  $0 < r < 1$ , the co-polarized phase difference contains information on the stratified medium. In [17], we also showed that outside the incidence plane and when  $r \neq 1$ , the phase difference between two cross-polarized signals for single-look signatures is not uniformly distributed and contains information on the multilayer stack

Here, we are focused on the statistical properties of the co-polarized and cross-polarized phase differences but for multilook signatures. The next section gives the statistical properties of the stratified medium under study. In Section 3,

This is an open access article under the terms of the Creative Commons Attribution License, which permits use, distribution and reproduction in any medium, provided the original work is properly cited.

© 2021 The Authors. *IET Microwaves, Antennas & Propagation* published by John Wiley & Sons Ltd on behalf of The Institution of Engineering and Technology.

we derive the joint probability distribution of the scattering amplitudes from the random surface properties. The scattering amplitudes are obtained from the first-order perturbation theory [18–27]. In Section 4, supplemented by an appendix, we derive the closed-form expression for the PDF of the co-polarized and cross-polarized phase differences. The validation of the analytical formulas by comparison with Monte-Carlo results is reported in Section 5.

## 2 | PROBLEM GEOMETRY

The geometry of Figure 1 includes interfaces one ( $z = a_1(x, y)$ ) and two ( $z = -u_0 + a_2(x, y)$ ) resulting in three homogeneous regions. The average thickness of the central layer is denoted by  $u_0$ . The surface PDFs are Gaussian and centred. For the numerical applications, the spectrum of each interface is Gaussian and given by Equation (1) with  $i = j$ . The cross-spectrum is given by Equation (1) with  $i = 1$  and  $j = 2$ .

$$\hat{R}_{ij}(\alpha, \beta) = q_{ij}\sigma_i\sigma_j\pi\sqrt{l_{xi}l_{xj}l_{yi}l_{yj}} \times \exp\left[-\alpha^2\frac{(l_{xi}^2 + l_{xj}^2)}{8} - \beta^2\frac{(l_{yi}^2 + l_{yj}^2)}{8}\right] \quad (1)$$

A function symbol with a superscript ‘‘ $\hat{\cdot}$ ’’ stands for the Fourier transform of the function. The quantities  $l_{xi}$  and  $l_{yi}$  designate the correlation lengths of the  $i$ -th interface and the quantity  $\sigma_i$  is the standard deviation of the  $i$ -th interface heights. If both correlation lengths are equal, the interface is isotropic else the interface is anisotropic. The coefficient  $q_{ij}$  is a mixing parameter with  $q_{ii} = 1$  and  $|q_{12}| \leq 1$  [22]. The correlation coefficient  $\rho_{12}$  is defined as the ratio of the cross-correlation function at the origin to the product of the standard deviations of heights and we find:

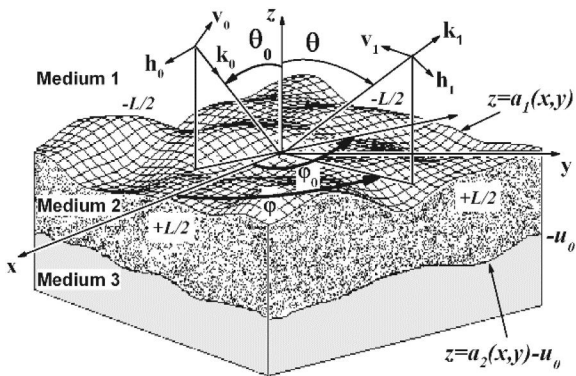


FIGURE 1 Geometry of 3-D scattering from a two-rough boundary layered structure

$$\rho_{12} = \frac{2q_{12}\sqrt{l_{x1}l_{x2}l_{y1}l_{y2}}}{\sqrt{(l_{x1}^2 + l_{x2}^2)(l_{y1}^2 + l_{y2}^2)}} \quad (2)$$

The two rough interfaces are not correlated when  $\rho_{12} = 0$ . If not, they are fully or partially correlated.

As shown in Figure 1, the stratified medium is illuminated by a monochromatic plane wave with a wavelength  $\lambda$ , under a horizontal (h) or a vertical (v) polarization. The direction of the incident wave vector  $k_0$  is defined by the angles  $\theta_0$  and  $\varphi_0$ . The inhomogeneous structure is composed of three different homogeneous non-magnetic regions: the air (medium 1), the upper ground layer (medium 2) and the lower ground layer (medium 3). The  $m$ -th region is characterized by a relative permittivity  $\epsilon_{rm}$ .

## 3 | SCATTERING AMPLITUDES AS A COMPLEX RANDOM PROCESSES

Within the validity region of the first-order SPM, the co-scattering and cross-scattering amplitudes  $A_{(ba)}^{(1)}(\theta, \varphi)$  within the upper medium take the following form [22]:

$$A_{(ba)}^{(1)}(\theta, \varphi) = K_{1,(ba)}(\alpha, \beta)\hat{a}_1(\alpha - \alpha_0, \beta - \beta_0) + K_{2,(ba)}(\alpha, \beta)\hat{a}_2(\alpha - \alpha_0, \beta - \beta_0) \quad (3)$$

where  $\alpha = k_1 \sin\theta \cos\varphi$ ,  $\beta = k_1 \sin\theta \sin\varphi$ ,  $\alpha_0 = k_1 \sin\theta_0 \cos\varphi_0$ ,  $\beta_0 = k_1 \sin\theta_0 \sin\varphi_0$  and  $k_1 = 2\pi/\lambda$ . The quantity  $k_1$  designates the wave-number in the medium 1. The angles  $\theta$  and  $\varphi$  define the direction of observation. The superscript (1) refers to the first-order SPM. The subscript (a) designates the impinging wave polarization (h or v) and the subscript (b), the scattered wave polarization (h or v), respectively. As shown in [22], the first-order SPM kernels  $K_{1,(ba)}(\alpha, \beta)$  and  $K_{2,(ba)}(\alpha, \beta)$  depend on the central layer thickness, on the relative permittivity values and on the incidence and scattering angles.

For a stack of homogeneous layers with randomly rough surfaces, the scattering amplitude  $A_{(ba)}^{(1)}(\theta, \varphi)$  depends on rough interface realizations and for a given direction  $(\theta, \varphi)$ , it is a complex random variable. Let  $R_{(ba)}$  and  $J_{(ba)}$  be the real and imaginary parts of the scattering amplitude  $A_{(ba)}^{(1)}(\theta, \varphi)$  and let  $R_{(b'a')}$  and  $J_{(b'a')}$  be the real and imaginary parts of  $A_{(b'a')}^{(1)}(\theta, \varphi)$ , respectively. We recall that the surface height distributions are assumed to be centred and Gaussian. As shown by Equation 3, the scattering amplitude is expressed as a linear combination of the Fourier transforms of the rough interface height profiles. Since the Gaussian character is preserved by linear operation, the two-dimensional Fourier transforms of  $a_1(x, y)$  and  $a_2(x, y)$  as well as the scattering amplitudes are Gaussian processes and we deduce that the four random variables  $R_{(ba)}$ ,  $J_{(ba)}$ ,  $R_{(b'a')}$  and  $J_{(b'a')}$  follow a four-order Gaussian distribution. Because the

rough interface height distributions are centred, the four random variables are also centred. In [16], we showed that the random variables  $R_{(ba)}$  and  $J_{(ba)}$  (respectively,  $R_{(b'a')}$  and  $J_{(b'a')}$ ) are not correlated when  $L \rightarrow \infty$ . They also have the same variance  $\sigma_{R_{ba}}^2$  (respectively,  $\sigma_{R_{b'a'}}^2$ ). Moreover, the random variables  $R_{(ba)}$  and  $R_{(b'a')}$  are correlated with a covariance  $\Gamma_{R_{ba}R_{b'a'}}$  while the random variables  $R_{(ba)}$  and  $J_{(b'a')}$  are correlated with a covariance  $\Gamma_{R_{ba}J_{b'a'}}$ . These variances and covariances are given by:

$$\sigma_{R_{ba}}^2 = \frac{1}{2} \sum_{i=1}^2 \sum_{j=1}^2 \operatorname{Re} \left[ K_{i,(ba)}^* K_{j,(ba)} \hat{R}_{ij}(\alpha - \alpha_0, \beta - \beta_0) \right] \quad (4)$$

$$\Gamma_{R_{ba}R_{b'a'}} = \frac{1}{2} \sum_{i=1}^2 \sum_{j=1}^2 \operatorname{Re} \left[ K_{i,(ba)}^* K_{j,(b'a')} \hat{R}_{ij}(\alpha - \alpha_0, \beta - \beta_0) \right] \quad (5)$$

$$\Gamma_{R_{ba}J_{b'a'}} = \frac{1}{2} \sum_{i=1}^2 \sum_{j=1}^2 \operatorname{Im} \left[ K_{i,(ba)}^* K_{j,(b'a')} \hat{R}_{ij}(\alpha - \alpha_0, \beta - \beta_0) \right] \quad (6)$$

Let  $M_{ba}$  and  $\Phi_{ba}$  be the modulus and phase of  $A_{(ba)}^{(1)}(\theta, \varphi)$  ( $M_{b'a'}$  and  $\Phi_{b'a'}$  for  $A_{(b'a')}^{(1)}(\theta, \varphi)$ , respectively). As shown in [16], by using polar coordinates, the joint PDF of these four random variables is determined as follows:

$$\begin{aligned} & \mathcal{P}_{M_{ba}, M_{b'a'}, \Phi_{ba}, \Phi_{b'a'}}(m_{ba}, m_{b'a'}, \phi_{ba}, \phi_{b'a'}) \\ &= \frac{m_{ba} m_{b'a'}}{4\pi^2 \sigma_{R_{ba}}^2 \sigma_{R_{b'a'}}^2 (1-r^2)} \\ & \times \exp \left[ -\frac{1}{2(1-r^2)} \left( \frac{m_{ba}^2}{\sigma_{R_{ba}}^2} - 2 \frac{m_{ba} m_{b'a'}}{\sqrt{\sigma_{R_{ba}}^2 \sigma_{R_{b'a'}}^2}} \zeta + \frac{m_{b'a'}^2}{\sigma_{R_{b'a'}}^2} \right) \right] \end{aligned} \quad (7)$$

where

$$\zeta = r \cos(\phi_{ba} - \phi_{b'a'} + \psi) \quad (8)$$

The angle  $\psi$  called the reference angle, which is defined by:

$$\psi = \tan^{-1} \left( \frac{\Gamma_{R_{ba}J_{b'a'}}}{\Gamma_{R_{ba}R_{b'a'}}} \right) \quad (9)$$

The modulus  $r$  of the correlation coefficient between the complex random variables  $A_{(ba)}^{(1)}(\theta, \varphi)$  and  $A_{(b'a')}^{(1)}(\theta, \varphi)$  is expressed as follows [16, 17]:

$$r = \sqrt{\frac{\Gamma_{R_{ba}R_{b'a'}} + \Gamma_{R_{ba}J_{b'a'}}}{\sigma_{R_{ba}}^2 \sigma_{R_{b'a'}}^2}} \quad (10)$$

Through the variances and covariances are given by Equations (4)–(6), the two parameters  $\psi$  and  $r$  given by Equations (9) and (10) depend on the spectra of random surfaces and on their cross-spectrum. For the numerical applications, the spectra and the cross-spectrum are Gaussian. Nevertheless, we have to keep in mind that the analytical approach presented here could be applied to any correlation function which vanishes at infinity. A sufficient condition for the existence of the Fourier transform of the statistical correlation function (i.e. the spectrum or the cross-spectrum) is that the correlation function limit is zero at infinity. In this case, the modulus of the correlation coefficient and the reference angle are defined.

The two parameters  $\psi$  and  $r$  also depend on the first-order SPM kernels that are related to the medium geometric and electromagnetic properties. These quantities change with the number of interfaces. J.M. Elson is one of the first authors to develop a vector theory of scattering from a stack of two-dimensional slightly rough interfaces. This vector theory allows the scattered intensity to be determined and can be used with partially correlated or uncorrelated surfaces. But, the analytical expressions of the first-order SPM kernels for a stratified medium with two rough interfaces were obtained for the first time in [19]. First-order SPM kernels for an arbitrary number of rough interfaces were originally established in closed-form in [20]. In [22] and [24], equivalent expressions have also been derived from a formalism based on the first-order perturbation of Rayleigh integrals. In [25, appendix A], for the first time, the analytical expressions giving the first-order SPM kernels as functions of the layer thicknesses, the relative permittivity values and of the incidence and scattering angle are established for a stratified medium with three rough interfaces. For an arbitrary number of interfaces, once the SPM kernels determined, the variances and covariances given by Equations (4) to (6) are calculated from summations over  $N$  surfaces and the parameters are obtained from Equations (9) and (10).

In [8–13], the statistics of single-look and multilook phase differences have been found under the hypothesis that the real and imaginary parts of the scattering amplitudes under consideration follow a Gaussian joint distribution. These works are based on a-priori assumption. For infinite slightly rough interfaces described by Gaussian centred stochastic processes, we demonstrate this property within the scope of the first-order SPM. The Gaussian assumption is derived from the statistics of the illuminated rough-interfaces layered medium and the parameters of the phase difference distribution are related to the geometric medium and electromagnetic properties.

The co-polarized and cross-polarized scattering amplitudes are expressed as linear combinations of the Fourier transforms of the surface height profiles. The weights of the linear combinations are the first-order SPM kernels. Since the Gaussian character is preserved by linear operation, the real and imaginary parts of the first order scattering amplitudes are Gaussian processes. This reasoning was used to derive the single-look phase difference statistics [16, 17]. In Section 4,

supplemented by an appendix, we derive, by coupling this idea to the work published in [11], the probability law of the multilook phase difference. This will allow the analysis of stratified grounds with slightly rough interfaces. To our knowledge, such work has not been done to date.

#### 4 | SINGLE-LOOK AND MULTILOOK PHASE DIFFERENCE DISTRIBUTIONS

The phase difference  $\Delta\Phi_{(ba,b'a')}$  between the two complex random variables  $A_{(ba)}^{(1)}$  and  $A_{(b'a')}^{(1)}$  is defined by,

$$\Delta\Phi_{(ba,b'a')} = \Phi_{(ba)} - \Phi_{(b'a')} = \arg(A_{(ba)}^{(1)} \cdot A_{(b'a')}^{(1)*}) \quad (11)$$

and the multilook phase difference  $\Delta\Phi_{(ba,b'a'),n}$  by,

$$\Delta\Phi_{(ba,b'a'),n} = \arg\left[\frac{1}{n} \sum_{i=1}^n A_{(ba),i}^{(1)} \cdot A_{(b'a'),i}^{(1)*}\right] \quad (12)$$

where the symbol ‘arg’ designates the argument of the quantity. We assume that the complex random variables  $(A_{(ba),i}^{(1)}, A_{(b'a'),i}^{(1)})$  and  $(A_{(ba),i \neq j}^{(1)}, A_{(b'a'),i \neq j}^{(1)})$  are independent and identically distributed (IID).

For multilook polarimetric signatures, the phase difference distribution has been derived from different approaches [11–14]. The derivation proposed in the appendix is based on Chapter 8 of the book [28] and on the appendix of [11]. The calculation is not straightforward and we made the choice to detail the different stages of the demonstration. The difference with respect to [11] is that we use the properties of the Fourier transform and not those of the Laplace transform. We find the phase difference PDF for multilook signatures and is as follows:

$$\begin{aligned} p_{\Delta\Phi_{(ba,b'a'),n}}(\Delta\phi) &= \frac{(1-r^2)^n}{2\pi} \\ &\times \left[ F\left(n; 1; 1/2; \zeta^2\right) \right. \\ &\left. + \zeta \frac{\pi}{2^n} \frac{(2n-1)!!}{\Gamma(n)} \frac{1}{(1-\zeta^2)^{n+1/2}} \right] \end{aligned} \quad (13)$$

where  $(2n-1)!! = (2n-1)(2n-3)\dots 3 \times 1$ . The special function  $F(a,b;c;d)$  is the Gauss hypergeometric function and the letter  $\Gamma$  designates the gamma function. Knowing that  $\Gamma(n+1/2) = (2n+1)!!/2^n \pi$ , we obtain the expression (18) in [13].

Knowing that  $F(a,b;c;0) = 1$  when  $\zeta = 0$ , i.e. when  $r = 0$ , the phase difference is uniformly distributed between 0 and  $2\pi$  for any number of looks. When  $r = 1$ , the phase difference is a deterministic quantity equal to  $-\psi$  (modulo  $[2\pi]$ ). The formula (13) is valid for an arbitrary number of looks. By using the properties of the Gauss hypergeometric function [29], we derive the  $n$ -look distribution for  $n = 1, 2, 3$  and 4 and we

obtain the analytical expressions (14) to (17), respectively. Also, when  $n \geq 5$ , more complicated algebraic expressions are obtained. For this reason, we have restricted ourselves to the first four values of  $n$ .

$$\begin{aligned} p_{\Delta\Phi_{(ba,b'a'),1}}(\Delta\phi) &= \frac{(1-r^2)}{2\pi(1-\zeta^2)} \\ &\times \left[ 1 + \frac{\zeta}{\sqrt{1-\zeta^2}} \left( \frac{\pi}{2} + \arctan \frac{\zeta}{\sqrt{1-\zeta^2}} \right) \right] \end{aligned} \quad (14)$$

$$\begin{aligned} p_{\Delta\Phi_{(ba,b'a'),2}}(\Delta\phi) &= \frac{(1-r^2)^2}{4\pi(1-\zeta^2)^2} \\ &\times \left[ 2 + \zeta^2 + \frac{3\zeta}{\sqrt{1-\zeta^2}} \left( \frac{\pi}{2} + \arctan \frac{\zeta}{\sqrt{1-\zeta^2}} \right) \right] \end{aligned} \quad (15)$$

$$\begin{aligned} p_{\Delta\Phi_{(ba,b'a'),3}}(\Delta\phi) &= \frac{(1-r^2)^3}{16\pi(1-\zeta^2)^3} \\ &\times \left[ 8 + 9\zeta^2 - 2\zeta^4 + \frac{15\zeta}{\sqrt{1-\zeta^2}} \left( \frac{\pi}{2} + \arctan \frac{\zeta}{\sqrt{1-\zeta^2}} \right) \right] \end{aligned} \quad (16)$$

$$\begin{aligned} p_{\Delta\Phi_{(ba,b'a'),4}}(\Delta\phi) &= \frac{(1-r^2)^4}{96\pi(1-\zeta^2)^4} \left[ 48 + 87\zeta^2 - 38\zeta^4 + 8\zeta^6 \right. \\ &\left. + \frac{105\zeta}{\sqrt{1-\zeta^2}} \left( \frac{\pi}{2} + \arctan \frac{\zeta}{\sqrt{1-\zeta^2}} \right) \right] \end{aligned} \quad (17)$$

Knowing that  $\arcsin\zeta = \arctan \frac{\zeta}{\sqrt{1-\zeta^2}}$  for  $-1 < \zeta < 1$  and that  $\arcsin\zeta = \pi/2 - \arccos\zeta$ , we obtain the closed-form expressions (21) to (24) published in [13].

#### 5 | NUMERICAL RESULTS

The formula (13) giving the multilook phase difference distribution can be used for an arbitrary number of interfaces. The authors in their work have chosen to present results for stratified structures with two interfaces, but the validation has been carried out for configurations with three and four random interfaces and the reason that we have applied regardless of the number of interfaces. The theoretical formulae are verified by comparison with Monte-Carlo simulations.

We consider a two-layer rough ground [30]. The relative permittivity values are  $\epsilon_{r2} = 4.66 - 0.29j$  and  $\epsilon_{r3} = 8.75 - 0.85j$  at 1.25 GHz [31]. The standard deviations of the surface heights are  $\sigma_1 = 0.5$  cm and  $\sigma_2 = 0.4$  cm. The thickness  $u_0$  of the central layer is equal to 5 cm [32]. The first interface is anisotropic with  $l_{x1} = 5$  cm and  $l_{y1} = 4$  cm. The second one is isotropic with  $l_{x2} = l_{y2} = 6$  cm. The correlation coefficient

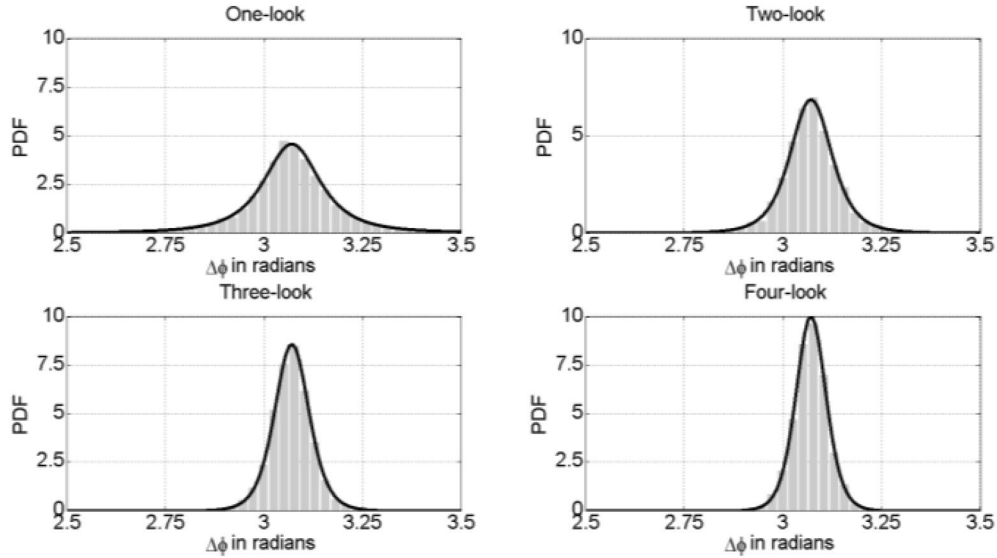


FIGURE 2 PDF of the co-polarized phase difference in the backscattering configuration and the associated histogram for  $n = 1, 2, 3$  and  $4$

between both interfaces is equal to 0.2. The two-rough boundary layered structure is illuminated by a plane wave under  $\theta_0 = 30^\circ$  and  $\varphi_0 = 0^\circ$ . The theoretical PDFs given by Equations (14) to (17) are compared with histograms obtained from Monte-Carlo simulations. The histograms are obtained from  $2^{13}$  values of difference phase deduced from the scattering amplitudes given by Equation (3). The Fourier transforms of the rough interface functions  $a_1(x, y)$  and  $a_2(x, y)$  are estimated on areas of  $400\lambda^2$ . The rough surface realizations are generated by Gaussian filters applied to uncorrelated white Gaussian noise realizations in [25].

We consider the co-polarized phase difference  $\Delta\Phi_{(bh,vv),n}$  in the backscattering configuration and the cross-polarized phase difference  $\Delta\Phi_{(bv,vv),n}$  in the transverse plane with  $\theta = -\theta_0$  and  $\varphi = 90^\circ$ .

Figure 2 shows the PDF of the co-polarized phase difference  $\Delta\Phi_{(bh,vv),n}$  for  $n = 1, 2, 3$  and  $4$ . The agreement between the theoretical probability laws and the Monte-Carlo simulations is very good. For each value of  $n$ , the comparison validates the theory for the co-polarized phase difference in the backscattering direction. Given the used parameters, the co-polarized complex amplitudes  $A_{(bh)}^{(1)}$  and  $A_{(vv)}^{(1)}$  are strongly correlated with  $r = 0.994$ . The reference angle  $\psi$  is equal to 3.13 rad. Table 1 gives the mean and standard deviation (STD) of  $\Delta\Phi_{(bh,vv),n}$  for each number of looks. When this number increases, the mean remains unchanged but the STD decreases in accordance with the averaging effect of the multilook processing. As a result, the PDF curve becomes narrower and the maximum value increases.

Figure 3 shows the theoretical PDF of  $\Delta\Phi_{(bv,vv),n}$  and the associated histogram for the four values of  $n$ . As previously, we find a very good agreement. Given the used parameters, the complex signals  $A_{(bv)}^{(1)}$  and  $A_{(vv)}^{(1)}$  are strongly correlated with  $r = 0.872$ . The reference angle  $\psi$  is equal to 3.37 rad. As shown in Table 2, when the number of looks increases, the mean of  $\Delta\Phi_{(bv,vv),n}$  varies very slightly but the value of the standard

TABLE 1 Values of the mean and standard deviation of  $\Delta\Phi_{(bh,vv),n}$

$n$	1	2	3	4
Mean in rad	3.07	3.07	3.07	3.07
STD in rad	0.0670	0.0250	0.0175	0.0142

deviation decreases and the probability distribution curve becomes narrower and the maximum value increases.

## 6 | CONCLUSION

We have derived the distribution of the phase difference between two scattering amplitudes for multilook polarimetric configurations characterizing rough boundary layered structures illuminated by a plane wave. In the first stage, for infinite slightly rough surfaces described by Gaussian centred stochastic processes, we show that the real and imaginary parts of the two complex scattering amplitudes follow a Gaussian joint distribution. We demonstrate this property in the context of the first-order perturbation theory. In a second stage, we derive from this joint distribution the closed-form formula for the probability law of the phase difference. The phase difference PDF is expressed in terms of the Gauss hypergeometric functions and only depends on the number of looks  $n$ , the correlation coefficient  $r$  between the scattering amplitudes under study and a reference phase  $\psi$ .

For two-rough boundary layered ground, the theoretical PDF is validated by a comparison with the histogram derived from Monte-Carlo simulations in both monostatic and bistatic configurations. We note that when the number of looks increases, the mean of the co-polarized or cross-polarized phase difference is unchanged but the standard deviation decreases in accordance with the averaging effect of the multilook processing.

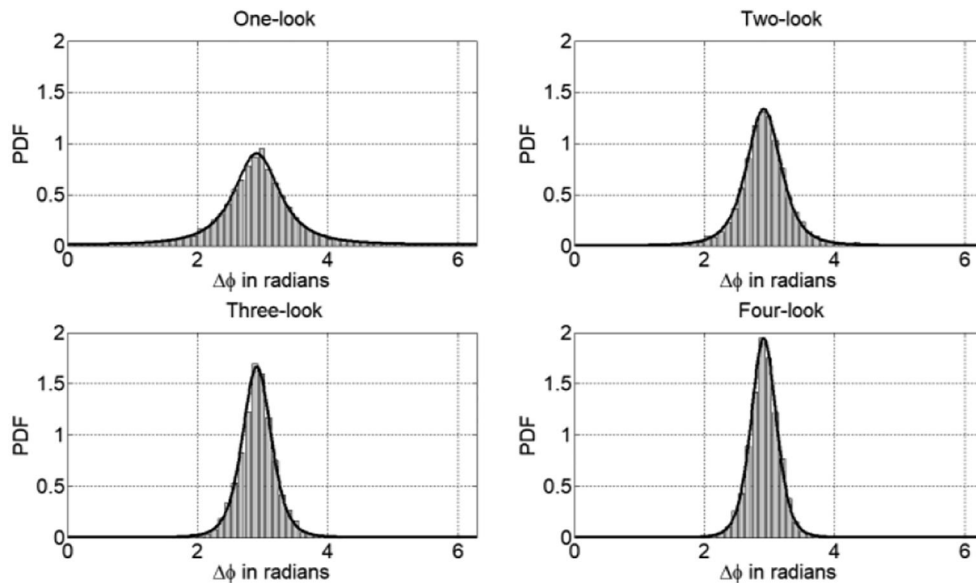


FIGURE 3 PDF of  $\Delta\Phi_{(bv,rv),n}$  and the associated histogram in the transverse plane for  $n = 1, 2, 3$  and  $4$

TABLE 2 Values of the mean and the standard deviation of  $\Delta\Phi_{(bv,rv),n}$

$n$	1	2	3	4
Mean in rad	2.94	2.92	2.92	2.91
STD in rad	0.779	0.434	0.315	0.241

For slightly rough surfaces described by Gaussian centred stochastic processes and within the SPM scope, we have established the joint probability density function for the scattering amplitudes and the probability density function for the co-polarized and cross-polarized phase differences because the Gaussian character is preserved by linear operation. For a non-Gaussian rough surface, we do not know how to conclude on the nature of the joint probability law of the real and imaginary parts of the scattering amplitudes. The Gaussian character is not systematically observed on soil surfaces. For example, the height distribution of some ploughed soils is not Gaussian [33–35]. It therefore appears useful to derive the analytical expression for the statistical distribution of the phase difference within the framework of the small perturbation method. It is an open question and deserves a complete analysis.

## ORCID

Richard Dusséaux  <https://orcid.org/0000-0003-3194-9158>

## REFERENCES

1. Ulaby, F.T., Elachi, C.: Radar Polarimetry for Geoscience Applications. pp. 1–376. Attech House, Norwood, MA (1990)
2. Ulaby, F.T., et al.: Relating polarization phase difference of SAR signals to scene properties. *IEEE Trans. Geosci. Rem. Sens.* 25(1), 83–92 (1987)
3. Lasne, Y., et al.: A phase signature for detecting wet subsurface structures using polarimetric L-band SAR. *IEEE Trans. Geosci. Rem. Sens.* 42(8), 1683–1694 (2004)
4. Lasne, Y., et al.: Effect of multiple scattering on phase signature of buried wet subsurface structures: applications to polarimetric L and C-band SAR. *IEEE Trans. Geosci. Rem. Sens.* 43(8), 1716–1726 (2005)
5. Migliaccio, M., Nunziata, F., Gambardella, A.: On the co-polarized phase difference for oil spill observation. *Int. J. Remote Sens.* 30(6), 1587–1602 (2009)
6. Nunziata, F., Gambardella, A., Migliaccio, M.: A unitary Mueller-based view of polarimetric SAR oil slick observation. *Int. J. Remote Sens.* 33(20), 6403–6425 (2012)
7. Haldar, D., et al.: Analysis of temporal polarization phase difference for major crops in India. *Progr. Electromagn. Res. B*, 57, 299–309 (2014)
8. Kong, J.A., et al.: Identification of terrain cover using the optimum polarimetric classifier. *J. Electromagnet. Wave. Appl.* 8(2), 171–194 (1987)
9. Eom, H.J., and Boerner, W-M.: Statistical properties of the phase difference between two orthogonally polarized SAR signals. *IEEE Trans. Geosci. Rem. Sens.* 29(1), 182–183 (1991)
10. Sarabandi, K.: Derivation of phase statistics from the Mueller matrix. *Radio Sci.*, 27(5), 553–560 (1992)
11. Joughin, I.R., Winebrenner, D.P., Percival, D.B.: Probability density functions for multilook polarimetric signatures. *IEEE Trans. Geosci. Rem. Sens.* 32(3), 562–574 (1994)
12. Lee, J.S., Miller, A.R., Hoppel, K.W.: Statistics of phase difference and product magnitude of multi-look processed Gaussian signals. *Waves Random Media*, 4, 307–319 (1994)
13. Lee, J.S., et al.: Intensity and phase statistics of multilook polarimetric and interferometric SAR imagery. *IEEE Trans. Geosci. Rem. Sens.* 32(5), 1017–1028 (1994)
14. Touzi, R., Lopes, A.: Statistics of the Stokes parameters and of the complex coherence parameters in one-look and multilook speckle fields. *IEEE Trans. Geosci. Rem. Sens.* 34(2), 519–531 (1996)
15. Lee, J.-S., Pottier, E.: *Polarimetric Radar Imaging: From Basics to Applications*. pp. 1–398. CRC Press, Boca Raton, FL (2009)
16. Afifi, S., Dusséaux, R.: On the co-polarized phase difference of rough layered surfaces: Formulas derived from the small perturbation method. *IEEE Trans. Antennas Propag.* 59(7), 2607–2618 (2011)
17. Dusséaux, R., Afifi, S.: Statistical distributions of the co- and cross-polarized phase differences of stratified media. *IEEE Trans. Antennas Propag.* 65(3), 1517–1521 (2017)

18. Elson, J.M.: Infrared light scattering from surfaces covered with multiple dielectric overlayers. *Appl. Opt.* 16(11), 2873–2881 (1977)
19. Tabatabaenejad, A., Moghaddam, M.: Bistatic scattering from three-dimensional layered rough surfaces. *IEEE Trans. Geosci. Rem. Sens.* 44(8), 2102–2114 (2006)
20. Imperatore, P., Iodice, A., Riccio, D.: Electromagnetic wave scattering from layered structures with an arbitrary number of rough interfaces. *IEEE Trans. Geosci. Rem. Sens.* 47(4), 1056–1072 (2009)
21. Imperatore, P., et al.: Modelling scattering of electromagnetic waves in layered media: an up-to-date perspective. *Int. J. Antenna. Propag.* 1–14 (2017)
22. Afifi, S., Dusséaux, R.: Scattering by anisotropic rough layered 2D interfaces. *IEEE Trans. Antenna. Propag.* 60(11), 5315–5328 (2012)
23. Berrouk, A., Dusséaux, R., Afifi, S.: Electromagnetic wave scattering from rough layered interfaces: analysis with the small perturbation method and the small slope approximation. *Progr. Electromagn. Res. B*, 57, 177–190 (2014)
24. Afifi, S., Dusséaux, R., Berrouk, A.: Electromagnetic scattering from 3D layered structures with randomly rough interfaces: Analysis with the small perturbation method and the small slope approximation. *IEEE Trans. Antennas Propag.* 62(10), 5200–5208 (2014)
25. Dusséaux, R., Afifi, S.: Statistical distribution of the Layered Rough Surface Index (LRSI). *Progr. Electromagn. Res. C*, 94, 75–87 (2019)
26. Zamani, H., Tavakoli, A., Dehmollaian, M.: Scattering from two rough surfaces with inhomogeneous dielectric profiles. *IEEE Trans. Antenna. Propag.* 63(12), 5753–5766 (2015)
27. Zamani, H., Tavakoli, A., Dehmollaian, M.: Scattering from layered rough surfaces: analytical and numerical investigations. *IEEE Trans. Geosci. Rem. Sens.* 54(6), 3685–3696 (2016)
28. Davenport, W.B., Root, W.L.: *An Introduction to the Theory of Random Signals and Noise*, pp. 1–393. McGraw-Hill, New York (1987)
29. Erdélyi, A., et al. *Higher Transcendental Functions Vol. 1*. NewYork McGraw-Hill (1953)
30. Dusséaux, R., Afifi, S.: Multilook intensity ratio distribution for 3D layered structures with slightly rough interfaces. *IEEE Trans. Antenna. Propag.* 68(7), 5575–5582 (2020)
31. Wang, J.R., Schmugge, T.J.: An empirical model for the complex dielectric permittivity of soils as a function of water content. *IEEE Trans. Geosci. Rem. Sens.* 18(4), 288–295 (1980)
32. Boisvert, J.B., et al.: Effect of surface soil moisture gradients on modelling radar backscattering from bare fields. *Int. J. Remote Sens.* 18(1), 153–170 (1997)
33. Braham, K.A.: *Diffusion des ondes électromagnétiques par des surfaces rugueuses aléatoires naturelles. Méthode exacte en coordonnées curvilignes et Principe du faible couplage*. PhD thesis, Université de Versailles-Saint-Quentin-en-Yvelines. pp. 1–176. Versailles, France (2007)
34. Dusséaux, R., et al.: Study of backscatter signature for seedbed surface evolution under rainfall—influence of radar precision. *Progr. Electromagn. Res.* 125, 415–437 (2012)
35. Vannier, E., et al.: Statistical characterization of bare soil surface microrelief. *Adv. Geosci. Remote Sens.* 207–228 (2014)
36. Gradshteyn, I.S., Ryzhik, I.M. *Table of Integrals, Series and Products*. 7, pp. 1–1159. Elsevier Academic Press Publications, San Diego, California (2007)
37. Watson, G.N.: *A Treatise on the Theory of Bessel Functions*. 1–794. Cambridge University Press, Cambridge (1995)

**How to cite this article:** Afifi S, Dusséaux R. Multilook phase difference distribution for slightly rough boundary layered ground. *IET Microw. Antennas Propag.* 2021;15:718–727. <https://doi.org/10.1049/mia2.12071>

## APPENDIX

In order to facilitate the derivation of the phase difference distribution, let us introduce two new random variables  $Z$  and  $Y$  [28, p.164 (8–105)],

$$\begin{aligned} M_{ba} &= \sqrt{\sigma_{R_{ba}}^2 (1 - r^2)} \sqrt{Z} \exp(Y) \\ M_{b'd'} &= \sqrt{\sigma_{R_{b'd'}}^2 (1 - r^2)} \sqrt{Z} \exp(-Y) \end{aligned} \quad (A1)$$

where

$$Z = \frac{M_{ba} M_{b'd'}}{\sigma_{R_{b'd'}}^2 (1 - r^2)} \quad (A2)$$

and

$$Y = \frac{1}{2} \ln \left( \frac{M_{ba}}{M_{b'd'}} \right) \quad (A3)$$

The magnitude of the Jacobian of the transformation from  $M_{ba}$  and  $M_{b'd'}$  to  $Z$  and  $Y$  is:

$$|J| = (1 - r^2) \sqrt{\sigma_{R_{ba}}^2 \sigma_{R_{b'd'}}^2} \quad (A4)$$

Using this transformation, we obtain from Equation (7) the joint PDF for the four random variables  $Z$ ,  $Y$ ,  $\Phi_{(ba)}$  and  $\Phi_{(b'd')}$ ,

$$\begin{aligned} p_{Z,Y,\Phi_{ba},\Phi_{b'd'}}(z, y, \phi_{ba}, \phi_{b'd'}) &= \frac{1 - r^2}{4\pi^2} \\ &\times z \exp\{-z[\cosh(2y) - \zeta]\} \end{aligned} \quad (A5)$$

where the domain of  $z$  is  $[0, +\infty[$  and that of  $y$  is  $]-\infty, +\infty[$ . Knowing that the modified Bessel function of the second kind  $K_0(z)$  is defined by:

$$K_0(z) = \int_{-\infty}^{+\infty} \exp[-z \cosh(2y)] dy \quad (A6)$$

we obtain the joint PDF for the three random variables  $Z$ ,  $\Phi_{(ba)}$  and  $\Phi_{(b'd')}$  by integrating  $p_{Z,Y,\Phi_{ba},\Phi_{b'd'}}(z, y, \phi_{ba}, \phi_{b'd'})$  over  $y$ ,

$$p_{Z,\Phi_{ba},\Phi_{b'd'}}(z, \phi_{ba}, \phi_{b'd'}) = \frac{1 - r^2}{4\pi^2} z \exp[+z\zeta] K_0(z) \quad (A7)$$

The joint PDF  $p_{Z,\Delta\Phi_{(ba,b'd')}}(z, \Delta\Phi_{(ba,b'd')})$  of the random variable  $Z$  and  $\Delta\Phi_{(ba,b'd')}$  is found from  $p_{Z,\Phi_{ba},\Phi_{b'd'}}$  by the following integral,

$$\begin{aligned}
& p_{Z, \Delta\Phi_{(ba, b'a')}}(z, \Delta\phi_{(ba, b'a')}) \\
&= \int_{-\pi}^{+\pi} p_{Z, \Phi_{ba}, \Phi_{b'a'}}(z, \Delta\phi_{(ba, b'a')} + \phi_{b'a'}, \phi_{b'a'}) d\phi_{b'a'} \quad (\text{A8}) \\
&= \frac{(1-r^2)}{2\pi} z \exp[+z\zeta] K_0(z)
\end{aligned}$$

We can derive the PDF for the single-look phase difference by integrating  $p_{Z, \Delta\Phi_{(ba, b'a')}}(z, \Delta\phi_{(ba, b'a')})$  over  $z$ . Here we define from  $p_{Z, \Delta\Phi_{(ba, b'a')}}(z, \Delta\phi_{(ba, b'a')})$  a new probability law that allows the derivation of the distribution of the phase difference for single-look and multilook polarimetric signatures.

We write from (A1) and (A2) the product  $A_{(ba)}^{(1)} \cdot A_{(b'a')}^{(1)*}$  as follows:

$$\begin{aligned}
A_{(ba)}^{(1)} \cdot A_{(b'a')}^{(1)*} &= (1-r^2) \sqrt{\sigma_{R_{ba}}^2 \sigma_{R_{b'a'}}^2} \\
&\times [Z \cos(\Delta\Phi_{(ba, b'a')}) + jZ \sin(\Delta\Phi_{(ba, b'a')})] \quad (\text{A9})
\end{aligned}$$

Let us introduce two new random variables,  $U$  and  $V$ ,

$$U = Z \cos(\Delta\Phi_{(ba, b'a')}); V = Z \sin(\Delta\Phi_{(ba, b'a')}) \quad (\text{A10})$$

where

$$Z = \sqrt{U^2 + V^2}; \Delta\Phi_{(ba, b'a')} = \arctan\left(\frac{V}{U}\right) \quad (\text{A11})$$

The magnitude of the Jacobian of the bijective transformation from  $U$  and  $V$  to  $Z$  and  $\Delta\Phi_{(ba, b'a')}$  is equal to  $z$  and we deduce the joint probability law for the two random variables  $U$  and  $V$  from (8) and (A8) as follows:

$$\begin{aligned}
p_{UV}(u, v) &= \frac{(1-r^2)}{2\pi} \\
&\times \exp\left[\frac{\Gamma_{R_{ba}R_{b'a'}}u - \Gamma_{R_{ba}I_{b'a'}}v}{\sqrt{\sigma_{R_{ba}}^2 \sigma_{R_{b'a'}}^2}}\right] K_0(\sqrt{u^2 + v^2}) \quad (\text{A12})
\end{aligned}$$

We derive the multilook phase difference distribution from the probability law  $p_{UV}(u, v)$  and by using the independence of the complex random variables  $(A_{(ba), i}^{(1)}, A_{(b'a'), i}^{(1)})$  and  $(A_{(ba), j \neq i}^{(1)}, A_{(b'a'), j \neq i}^{(1)})$ . Once the general probability law has been established for a multilook polarimetric signature, we apply this law with  $n=1$  to obtain the distribution for a single-look signature. In accordance with (12) and (A10), the multilook phase difference is:

$$\Delta\Phi_{(ba, b'a'), n} = \arg\left[\frac{1}{n} \sum_{i=1}^n A_{(ba), i}^{(1)} \cdot A_{(b'a'), i}^{(1)*}\right] = \arg[\bar{U}_n + j\bar{V}_n] \quad (\text{A13})$$

where

$$\bar{U}_n = \sum_{i=1}^n U_i; \bar{V}_n = \sum_{i=1}^n V_i \quad (\text{A14})$$

Insofar as the complex random variables  $(A_{(ba), i}^{(1)}, A_{(b'a'), i}^{(1)})$  and  $(A_{(ba), j \neq i}^{(1)}, A_{(b'a'), j \neq i}^{(1)})$  are IID, the two random variables  $\bar{U}_n$  and  $\bar{V}_n$  are defined as the sum of  $n$  IID random variables. So, the joint PDF  $p_{\bar{U}_n, \bar{V}_n}(\bar{u}_n, \bar{v}_n)$  is obtained by convolving  $p_{UV}(u, v)$  with itself  $n-1$  times. First, let's consider the convolution product of the function  $p_{UV}(u, v)$  with itself.

$$\begin{aligned}
p_{\bar{U}_2, \bar{V}_2}(\bar{u}_2, \bar{v}_2) &= (p_{UV} \otimes p_{UV})\left(\bar{u}_2, \bar{v}_2\right) \\
&= \int_{-\infty}^{+\infty} \int_{-\infty}^{+\infty} p_{UV}(u, v) \\
&\quad \times p_{UV}(\bar{u}_2 - u, \bar{v}_2 - v) dudv \quad (\text{A15})
\end{aligned}$$

where the symbol  $\otimes$  denotes the convolution product. By substituting (A12) into (A15), we find:

$$\begin{aligned}
p_{\bar{U}_2, \bar{V}_2}(\bar{u}_2, \bar{v}_2) &= \frac{(1-r^2)^2}{(2\pi)^2} \exp\left(\frac{\Gamma_{R_{ba}R_{b'a'}}\bar{u}_2 - \Gamma_{R_{ba}I_{b'a'}}\bar{v}_2}{\sqrt{\sigma_{R_{ba}}^2 \sigma_{R_{b'a'}}^2}}\right) \\
&\quad \times [K_0(\sqrt{u^2 + v^2}) \otimes K_0(\sqrt{u^2 + v^2})] \quad (\text{A16})
\end{aligned}$$

Similarly, we find the joint distribution  $p_{\bar{U}_n, \bar{V}_n}(\bar{u}_n, \bar{v}_n)$ ,

$$\begin{aligned}
p_{\bar{U}_n, \bar{V}_n}(\bar{u}_n, \bar{v}_n) &= \frac{(1-r^2)^n}{(2\pi)^n} \\
&\times \exp\left(\frac{\Gamma_{R_{ba}R_{b'a'}}\bar{u}_n - \Gamma_{R_{ba}I_{b'a'}}\bar{v}_n}{\sqrt{\sigma_{R_{ba}}^2 \sigma_{R_{b'a'}}^2}}\right) K_0^{(n)}(\bar{u}_n, \bar{v}_n) \quad (\text{A17})
\end{aligned}$$

where  $K_0^{(n)}(\bar{u}_n, \bar{v}_n) = [K_0\sqrt{u^2 + v^2}] \otimes \dots \otimes K_0\sqrt{u^2 + v^2}$  ( $\bar{u}_n, \bar{v}_n$ ).

The convolution product  $K_0^{(n)}(\bar{u}_n, \bar{v}_n)$  can be performed by using Fourier transforms and the convolution theorem. The two-dimensional Fourier transform of  $K_0(\sqrt{u^2 + v^2})$  is defined by:

$$\hat{K}_0(\tilde{u}, \tilde{v}) = \int_{-\infty}^{+\infty} \int_{-\infty}^{+\infty} K_0\left(\sqrt{u^2 + v^2}\right) \exp(-j\tilde{u}u - j\tilde{v}v) dudv \quad (\text{A18})$$

Transforming to polar coordinates with  $u = \rho \cos\theta$  and  $v = \rho \sin\theta$  leads to:

$$\hat{K}_0(\tilde{u}, \tilde{v}) = \int_0^{2\pi} \int_0^{+\infty} K_0(\rho) \exp(-j\rho\tilde{u}\cos\theta - j\rho\tilde{v}\sin\theta) \rho d\rho d\theta \quad (\text{A19})$$

Knowing that the Bessel function of the first kind is defined by:

$$J_0(z) = \frac{1}{2\pi} \int_{\phi}^{2\pi+\phi} \exp(-jz \sin\theta) d\theta \quad (\text{A20})$$

we find:

$$\hat{K}_0(\tilde{u}, \tilde{v}) = 2\pi \int_0^{+\infty} K_0(\rho) J_0\left(\rho\sqrt{\tilde{u}^2 + \tilde{v}^2}\right) \rho d\rho \quad (\text{A21})$$

By using the formula (36, p. 665, Equation (2)),

$$\int_0^{+\infty} x K_\nu(ax) J_\nu(bx) dx = \frac{b^\nu}{a^\nu (b^2 + a^2)} \quad (\text{A22})$$

where  $J_\nu(ax)$  and  $K_\nu(ax)$  designate the Bessel function of the first kind and the modified Bessel function of the second kind, we find:

$$\hat{K}_0(\tilde{u}, \tilde{v}) = \frac{2\pi}{(\tilde{u}^2 + \tilde{v}^2 + 1)} \quad (\text{A23})$$

By using the convolution theorem, we obtain the 2D Fourier transform  $\hat{K}_0^{(n)}(\tilde{u}_n, \tilde{v}_n)$  of  $K_0^{(n)}(\bar{u}_n, \bar{v}_n)$  as follows:

$$\hat{K}_0^{(n)}\left(\tilde{u}_n, \tilde{v}_n\right) = \frac{(2\pi)^n}{(\tilde{u}_n^2 + \tilde{v}_n^2 + 1)^n} \quad (\text{A24})$$

By using an inverse 2D Fourier transform, we find from (A24) that:

$$K_0^{(n)}\left(\bar{u}_n, \bar{v}_n\right) = \frac{1}{(2\pi)^2} \int_{-\infty}^{+\infty} \int_{-\infty}^{+\infty} \frac{(2\pi)^n}{(\tilde{u}_n^2 + \tilde{v}_n^2 + 1)^n} \times \exp\left(+j\tilde{u}_n\bar{u}_n + j\tilde{v}_n\bar{v}_n\right) d\tilde{u}_n d\tilde{v}_n \quad (\text{A25})$$

Using the polar coordinates  $\tilde{u}_n = \rho \cos\theta$  and  $\tilde{v}_n = \rho \sin\theta$  into (A25) leads to

$$K_0^{(n)}\left(\bar{u}_n, \bar{v}_n\right) = (2\pi)^{n-2} \times \int_0^{2\pi} \int_0^{+\infty} \frac{\exp\left[js\sqrt{\bar{u}_n^2 + \bar{v}_n^2} \cos(\theta - \chi_n)\right] \rho d\rho d\theta}{(\rho^2 + 1)^n} \quad (\text{A26})$$

where  $\chi_n = \arctan(\bar{v}_n/\bar{u}_n)$ . By using Formula (A20) given the zeroth-order Bessel function, we obtain:

$$K_0^{(n)}\left(\bar{u}_n, \bar{v}_n\right) = (2\pi)^{n-1} \int_0^{+\infty} \frac{\rho J_0(\rho\sqrt{\bar{u}_n^2 + \bar{v}_n^2})}{(\rho^2 + 1)^n} d\rho \quad (\text{A27})$$

Using the following formula (36, p. 678, Equation (4)),

$$\int_0^{+\infty} \frac{J_\nu(bs)s^{\nu+1}}{(s^2 + a^2)^{\mu+1}} ds = \frac{a^{\nu-\mu} b^\mu}{2^\mu \Gamma(\mu + 1)} K_{\nu-\mu}(ab) \quad (\text{A28})$$

where the letter  $\Gamma$  designates the Gamma function and using the parity of the  $\nu$  th-order modified Bessel function of the second kind, the function  $K_0^{(n)}(\bar{u}_n, \bar{v}_n)$  takes the following form:

$$K_0^{(n)}\left(\bar{u}_n, \bar{v}_n\right) = \frac{(\pi\sqrt{\bar{u}_n^2 + \bar{v}_n^2})^{n-1}}{\Gamma(n)} K_{n-1}\left(\sqrt{\bar{u}_n^2 + \bar{v}_n^2}\right) \quad (\text{A29})$$

Substituting this result into (A17) yields

$$\begin{aligned} p_{\bar{U}_n, \bar{V}_n}\left(\bar{u}_n, \bar{v}_n\right) &= \frac{(1-r^2)^n}{\pi 2^n \Gamma(n)} \sqrt{\bar{u}_n^2 + \bar{v}_n^2}^{2n-1} K_{n-1}\left(\sqrt{\bar{u}_n^2 + \bar{v}_n^2}\right) \\ &\times \exp\left[\frac{1}{\sqrt{\sigma_{R_{ba}}^2 \sigma_{R_{b'a'}}^2}} \left(\Gamma_{R_{ba}R_{b'a'}} \bar{u}_n - \Gamma_{R_{ba}I_{b'a'}} \bar{v}_n\right)\right] \quad (\text{A30}) \end{aligned}$$

By using the bijective transformation of  $(\bar{U}_n, \bar{V}_n)$  into  $(Z_n, \Delta\Phi_{(ba,b'a'),n})$  with  $\bar{U}_n = Z_n \cos(\Delta\Phi_{(ba,b'a'),n})$  and  $\bar{V}_n = Z_n \sin(\Delta\Phi_{(ba,b'a'),n})$ , we obtain from (A30) the joint PDF of  $Z_n$  and  $\Delta\Phi_{(ba,b'a'),n}$ :

$$\begin{aligned} p_{Z_n, \Delta\Phi_{(ba,b'a'),n}}(z_n, \Delta\phi_{(ba,b'a'),n}) &= \frac{(1-r^2)^n}{\pi 2^n \Gamma(n)} z_n^n K_{n-1}(z_n) \\ &\times \exp\left\{\frac{z_n \left[\Gamma_{R_{ba}R_{b'a'}} \cos(\Delta\phi_{(ba,b'a'),n}) - \Gamma_{R_{ba}I_{b'a'}} \sin(\Delta\phi_{(ba,b'a'),n})\right]}{\sqrt{\sigma_{R_{ba}}^2 \sigma_{R_{b'a'}}^2}}\right\} \quad (\text{A31}) \end{aligned}$$

We derive the PDF for the multilook phase difference by integrating  $p_{Z_n, \Delta\Phi(ba, b'a'), n}(z_n, \Delta\phi(ba, b'a'), n)$  over  $z$  and we obtain

$$p_{\Delta\Phi(ba, b'a'), n}(\Delta\phi(ba, b'a'), n) = \frac{(1-r^2)^n}{\pi 2^n \Gamma(n)} \times \int_0^{+\infty} z_n^n K_{n-1}(z_n) \exp(z_n \zeta_n) dz_n \tag{A32}$$

where  $\zeta_n$  is given by (13) with  $-1 < \zeta_n < +1$ . Using the following formula [37, Section 13.21 (7)],

$$\int_0^{+\infty} t^{\mu-1} e^{-t \cosh \alpha} K_\nu(t) dt = \sqrt{\frac{\pi}{2}} \Gamma(\mu - \nu) \Gamma(\mu + \nu) \times \frac{P_{\nu-1/2}^{1/2-\mu}(\cosh \alpha)}{\sinh^{\mu-1/2} \alpha} \tag{A33}$$

the multilook phase difference distribution becomes:

$$p_{\Delta\Phi(ba, b'a'), n}(\Delta\phi(ba, b'a'), n) = \frac{\Gamma(2n)}{\sqrt{2\pi} \Gamma(n)} \frac{(1-r^2)^n}{2^n} \times \left(\frac{1}{1-\zeta_n^2}\right)^{(n+1/2)/2} P_{n-3/2}^{-n-1/2}(-\zeta_n) \tag{A34}$$

where  $P_\nu^\mu(z)$  is the Legendre function of the first kind defined by (29, Section 3.2 (7)),

$$P_\nu^\mu(z) = \frac{2^\mu}{\Gamma(1-\mu)} \frac{1}{(1-z^2)^{\mu/2}} F\left(1-\mu+\nu, -\mu - \nu; 1-\mu; \frac{1-z}{2}\right) \tag{A35}$$

and  $F(a, b; c; d)$  is the Gauss hypergeometric function. By substituting (A35) into (A34), we find:

$$p_{\Delta\Phi(ba, b'a'), n}(\Delta\phi(ba, b'a'), n) = \frac{\Gamma(2n)}{\sqrt{2\pi} \Gamma(n)} \frac{(1-r^2)^n}{2^n} \frac{2^{-(n+1/2)}}{\Gamma\left(n + \frac{3}{2}\right)} \times F\left(2n; 2; n + \frac{3}{2}; \frac{1+\zeta_n}{2}\right) \tag{A36}$$

Finally, by using the following properties of the Gauss hypergeometric function,

$$F\left(2a, 2b; a+b+\frac{1}{2}; \frac{1+z}{2}\right) = \frac{\Gamma\left(a+b+\frac{1}{2}\right) \Gamma\left(\frac{1}{2}\right)}{\Gamma\left(a+\frac{1}{2}\right) \Gamma\left(b+\frac{1}{2}\right)} F\left(a, b; \frac{1}{2}; z^2\right) \tag{A37}$$

$$-z \frac{\Gamma\left(a+b+\frac{1}{2}\right) \Gamma\left(-\frac{1}{2}\right)}{\Gamma(a) \Gamma(b)} F\left(a+\frac{1}{2}, b+\frac{1}{2}; \frac{3}{2}; z^2\right)$$

and

$$F\left(n+\frac{1}{2}; \frac{3}{2}; \frac{3}{2}; \zeta_n^2\right) = \frac{1}{(1-\zeta_n^2)^{n+1/2}} \tag{A38}$$

the analytical expression for the multilook phase difference  $p_{\Delta\Phi(ba, b'a'), n}(\Delta\phi(ba, b'a'), n)$  is given by Formula (13).